

**Figure 2.** Fermi surfaces of the top three d-block bands with the same displacements as in Figure 1: (a) lower  $x^2 - y^2$  band; (b) upper  $x^2 - y^2$  band; (c)  $z^2 - y^2$  band.

Fermi surface, or partially filled with a 1D Fermi surface. Of course, partial filling of the  $z^2 - y^2$  band leads to partial emptying of the  $x^2 - y^2$  bands. Thus upon any O4 atom displacement that lowers the  $z^2 - y^2$  band below the Fermi level, the oxidation state of copper increases in the  $\text{CuO}_2$  layers from +2 to +2 +  $\Delta$  ( $\Delta$  small) but decreases in the  $\text{CuO}_3$  chains from +3 to +3 -  $\Delta$ . Therefore, certain lattice vibrational modes involving the O4 atom displacement will lead to slight valence fluctuations of the copper atoms.

Thus, slight displacement of the capping oxygen atom O4 from its equilibrium position gives rise to crucial changes in the band electronic structure of  $\text{YBa}_2\text{Cu}_3\text{O}_7$ . At room temperature the root-mean-square (rms) deviation of the O4 atom from its equilibrium position is about 0.09 Å,<sup>7</sup> and similar values have been reported at approximately 80 K.<sup>11,12</sup> Therefore, the O4 atom displacement on the order of  $\Delta x = \Delta y = \Delta z = 0.05$  Å should be easily accessible via the lattice vibration modes involving the O4 atoms. In the  $\text{CuO}_3$  chains, the rms deviation of the other oxygen atom (i.e., O1) is highly anisotropic and is much greater than that of the O4 atom<sup>7,12</sup> in the plane perpendicular to the Cu1-O1-Cu1 axis (e.g., 0.17, 0.06, and 0.16 Å, respectively, along the  $a$ ,  $b$ , and  $c$  axes at room temperature<sup>7</sup>). Our band calculations on  $\text{YBa}_2\text{Cu}_3\text{O}_7$  show that O1 atom displacements as large as 0.10 Å along either the  $a$  or the  $c$  axis hardly lower the  $z^2 - y^2$  band. Since O4 is much closer to Cu1 than is O1 (i.e., Cu1-O1 = 1.943 Å vs. Cu1-O4 = 1.850 Å<sup>7</sup>), the position of the  $z^2 - y^2$  band is primarily governed by the O4 atom displacement.

The present work shows that slight displacement of the capping oxygen atom (O4) from its equilibrium position gives rise to slight valence fluctuations of the copper atoms, interactions between two separated  $\text{CuO}_2$  layers within each  $\text{Ba}_2\text{Cu}_3\text{O}_{7-3}$  slab, and a change in the Fermi surface dimensionality of the  $\text{CuO}_3$  chain band. For the long-range order such as superconductivity to occur at a high temperature in each  $\text{Ba}_2\text{Cu}_3\text{O}_{7-3}$  slab, the copper atoms of the two separated  $\text{CuO}_2$  layers must interact effectively. Our study suggests that this can be easily achieved via the Cu2-O4-Cu1-O4-Cu2 bridges with the help of the lattice vibrational modes involving the capping oxygen atoms O4.

**Acknowledgment.** Work at North Carolina State University and Argonne National Laboratory was supported by the U.S. Department of Energy, Office of Basic Energy Sciences, Division of Materials Sciences, under Grant DE-FG05-86-ER45259 and under Contract W31-109-Eng-38, respectively. We express our appreciation for computing time made available by DOE on the ER-Cray X-MP computer.

- (11) Greedan, J. E.; O'Reilly, A.; Stager, C. V., submitted for publication in *Phys. Rev. B: Condens. Matter*.  
 (12) Capponi, J. J.; Chailout, C.; Hewat, A. W.; Lejay, P.; Marezio, M.; Nguyen, N.; Raveau, B.; Soubeyroux, J. L.; Tholence, J. L.; Tournier, R., submitted for publication in *Europhys. Lett.*

Department of Chemistry  
 North Carolina State University  
 Raleigh, North Carolina 27695-8204

Myung-Hwan Whangbo\*  
 Michel Evain

Chemistry and Materials Science  
 Divisions  
 Argonne National Laboratory  
 Argonne, Illinois 60439

Mark A. Beno  
 Jack M. Williams\*

Received April 16, 1987

## High- $T_c$ Superconductors: Selective Preparation and Characterization of Tetragonal and Orthorhombic (93 K Superconductor) Phases of $\text{YBa}_2\text{Cu}_3\text{O}_{7-x}$

Sir:

Dramatic milestones in terms of greatly increased superconducting transition temperatures have been achieved recently, resulting in  $T_c$ 's well above 90 K.<sup>1-3</sup> The materials in question were prepared from mixtures of  $\text{Y}_2\text{O}_3$ ,  $\text{BaCO}_3$ , and  $\text{CuO}$ , and the superconducting phase was subsequently identified as having the composition  $\text{YBa}_2\text{Cu}_3\text{O}_{9-\delta}$  ( $\delta \sim 2$ ).<sup>4</sup> X-ray powder patterns indicated that the compound had a perovskite-like structure,<sup>4,5</sup> similar to that found in some compositions of the La-Y-Ba-Cu-O system.<sup>6</sup> However, some confusion has arisen because two different structures, both presumably superconducting, have been reported for this material: a tetragonal phase ( $a = 3.85$  Å,  $c = 11.72$  Å, space group  $P4m2$ ) by means of single-crystal X-ray diffraction,<sup>7</sup> and an orthorhombic phase ( $a = 3.823$  Å,  $b = 3.886$  Å,  $c = 11.681$  Å, space group  $Pmmm$ )<sup>8</sup> from powder neutron diffraction studies.<sup>8-10</sup> Both structures are derived from a regular  $\text{ABX}_3$  perovskite by tripling the  $c$  axis concurrent with the ordering ...Y-Ba-Ba-Y-Ba-Ba... on the A site, but they differ in the specific oxygen vacancy arrangement, which, in turn, may depend on the method of preparation. Slow furnace cooling is reported to produce superconducting materials<sup>4,5,11</sup> with high  $T_c$ 's ( $\sim 90$  K), and the structure of this material is reportedly orthorhombic.<sup>8</sup> In this communication we report (i) the advantages of the coprecipitation method for the preparation of  $\text{YBa}_2\text{Cu}_3\text{O}_{7-x}$  ( $x \approx 0.1$ ) and also report (ii) that the two phases can be selectively obtained, i.e., orthorhombic or tetragonal, depending on the sample cooling rate subsequent to oxygen annealing, (iii) that superconductivity at 93 K exists only in the orthorhombic phase, and (iv) that the electrical properties of the tetragonal phase exhibit sample-to-sample variations ranging from a semiconductor to a lower  $T_c$  superconductor with a broad transition at  $\sim 60$  K.

For the preparation of  $\text{YBa}_2\text{Cu}_3\text{O}_{7-x}$ , we chose the "pH-adjusted carbonate route"<sup>12</sup> over the commonly used  $\text{Y}_2\text{O}_3$ - $\text{BaCO}_3$ - $\text{CuO}$  calcination method. The advantages of the former are several: (i) Y:Ba:Cu ratios in the final oxide are very close to the starting ratios (see below); (ii) better sample homogeneity (of the Y, Ba, Cu dispersion) results from this solution method than by grinding; (iii) virtually single-phase materials (with respect to composition) are obtained.

**Synthesis.** An aqueous solution (triply distilled water) of high purity  $\text{Y}(\text{NO}_3)_3$  (prepared from Y metal (99.99%) and concen-

- (1) Wu, M. K.; Ashburn, J. R.; Torng, C. J.; Hor, P. H.; Meng, R. L.; Gao, L.; Huang, Z. J.; Wang, Y. Q.; Chu, C. W. *Phys. Rev. Lett.* **1987**, *58*, 908.  
 (2) Chu, C. W.; Hor, P. H.; Meng, R. L.; Gao, L.; Huang, Z. J.; Wang, Y. Q.; Bechtold, J.; Campbell, D.; Wu, M. K.; Ashburn, J.; Huang, C. Y. *Phys. Rev. Lett.*, in press.  
 (3) Tarascon, J. M.; Greene, L. H.; McKinnon, W. R.; Hull, G. W. *Phys. Rev. Lett.*, in press.  
 (4) Cava, R. J.; Batlogg, B.; van Dover, R. B.; Murphy, D. W.; Sunshine, S.; Siegrist, T.; Remeika, J. P.; Rietman, E. A.; Zahurak, S.; Espinosa, G. P. *Phys. Rev. Lett.* **1987**, *58*, 1676.  
 (5) Grant, P. M.; Beyers, R. B.; Engler, E. M.; Lim, G.; Parkin, S. S. P.; Ramirez, M. L.; Lee, V. Y.; Nazzari, A.; Vazquez, J. E.; Savoy, R. J. *Phys. Rev. B: Condens. Matter*, in press.  
 (6) Er-Rakho, L.; Michel, C.; Provost, J.; Raveau, B.; *J. Solid State Chem.* **1981**, *37*, 151.  
 (7) Hazen, R. M.; Finger, L. W.; Angel, R. J.; Pewitt, C. T.; Ross, N. L.; Mao, H. K.; Hadjidakis, C. G.; Hor, P. H.; Meng, R. L.; Chu, C. W. *Phys. Rev. B: Condens. Matter*, in press.  
 (8) Beno, M. A.; Soderholm, L.; Capone, D. W., II; Hinks, D. G.; Jorgensen, J. D.; Schuller, I. K.; Segre, C. U.; Zhang, K.; Grace, J. D. *Appl. Phys. Lett.*, in press.  
 (9) Capponi, J. J.; Chailout, C.; Heuat, A. W.; Lejay, P.; Marezio, M.; Nguyen, N.; Raveau, B.; Soubeyroux, J. L.; Tholence, J. L.; Tournier, R. *Europhys. Lett.*, in press.  
 (10) Greedan, J. E.; O'Reilly, A.; Stager, C. V. *Phys. Rev.*, in press.  
 (11) Engler, E. M.; Lee, V. Y.; Nazzari, A. I.; Beyers, R. B.; Lim, G.; Grant, P. M.; Parkin, S. S. P.; Ramirez, M. L.; Vazquez, J. E.; Savoy, R. J. *J. Am. Chem. Soc.* **1987**, *109*, 2848.  
 (12) Wang, H. H.; Carlson, K. D.; Geiser, U.; Thorn, R. J.; Kao, H.-C. I.; Beno, M. A.; Monaghan, M. R.; Allen, T. J.; Prokosh, R. B.; Stupka, D. L.; Williams, J. M.; Flandermeyer, B. K.; Poeppel, R. B. *Inorg. Chem.* **1987**, *26*, 1474.

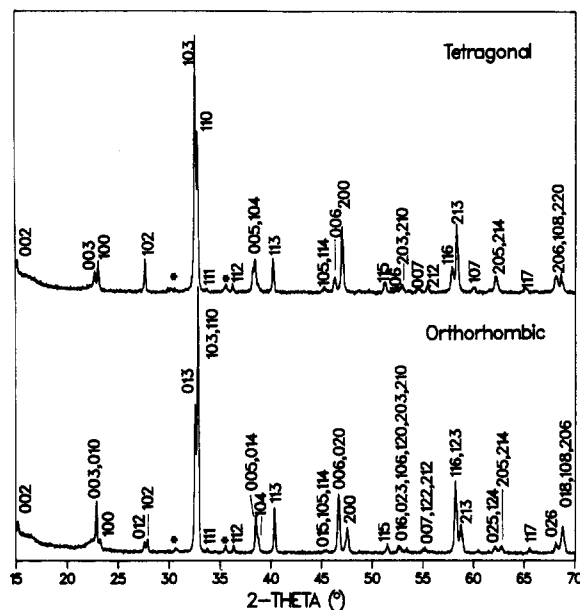


Figure 1. X-ray powder patterns ( $\lambda = 1.5418 \text{ \AA}$ ) of oxygen-annealed, fast-cooled tetragonal (top) and unannealed orthorhombic (bottom)  $\text{YBa}_2\text{Cu}_3\text{O}_{7-x}$ . Small impurities ( $\text{Y}_2\text{BaCuO}_5$  and  $\text{CuO}$ ) are marked with asterisks.

trated  $\text{HNO}_3$ ,  $\text{Ba}(\text{NO}_3)_2$ , and  $\text{Cu}(\text{NO}_3)_2 \cdot 3\text{H}_2\text{O}$  with a Y:Ba:Cu ratio of 1:2:3 is neutralized to pH  $\sim 7-8$  with KOH solution, and then a potassium carbonate solution (2–3-fold excess) is added. The precipitated hydroxy-carbonate mixture is centrifuged and washed until the filtrate pH stabilizes at  $\approx 9.7$ . Excessive washing after the pH reaches 9.7 should be avoided, since of the three metal carbonates,  $\text{BaCO}_3$  is slightly soluble in water ( $0.002 \text{ g}/100 \text{ cm}^3$ ). After being dried at  $120^\circ\text{C}$  overnight, the hydroxy-carbonate mixture is calcined in air at  $900^\circ\text{C}$  for 4 h in a muffle furnace producing a black powder, which, by powder X-ray diffraction, is virtually pure orthorhombic  $\text{YBa}_2\text{Cu}_3\text{O}_{7-x}$  with only very small amounts of impurities ( $\text{Y}_2\text{BaCuO}_5$  and  $\text{CuO}$ ). ICP/AES analysis of this oxide revealed the Y:Ba:Cu ratio to be 1:1.99:3.16 (error limits of the analysis  $\pm 5\%$ ).

Further annealing of compressed (ca. 30 000 psi) pellets of this black powder in a flowing oxygen atmosphere (ca  $7-10 \text{ S cm}^3/\text{min}$ ) at  $900-940^\circ\text{C}$  for 17–18 h is necessary to obtain the superconducting material ( $T_c > 90 \text{ K}$ ). These results have caused us, and others,<sup>4,11</sup> to believe that the oxygen content of this ternary oxide is a very important criterion for not only the  $T_c$  that will result but also the sharpness of the superconducting transition. Thus, while oxygen-annealed samples give superconductors with higher onset temperatures and a sharper transition, air-annealed samples give superconductors with a broad transition.

The effect of cooling rate of the oxygen-annealed samples on the resulting electrical properties is very dramatic. After oxygen annealing, if the sample is cooled rapidly by removing it from the oven into ambient air, the resultant material has a tetragonal structure (vide infra) as determined by X-ray powder diffraction. The electrical properties of the tetragonal phase were sample dependent, varying from a semiconductor to a superconductor with a lower  $T_c$  ( $T_c \sim 60 \text{ K}$ ), and this leads us to speculate that the actual oxygen content in the material is the origin of the variation in electrical properties. If, on the other hand, the oxygen-annealed sample is allowed to cool slowly ( $900-600^\circ\text{C}$  over 4 h,  $600-25^\circ\text{C}$  over 2–3 h) in an oxygen atmosphere, we obtain the orthorhombic phase, which is the 93 K superconductor. Sample-to-sample variations in the electrical properties of the oxygen-annealed, slow-cooled orthorhombic phase were relatively insignificant with  $T_c > 90 \text{ K}$  always being observed. Therefore, we conclude that the two different crystallographic phases that have been reported are due to different cooling rates during sample preparation. A recent high-temperature X-ray powder diffraction study has revealed that a reversible first order orthorhombic-

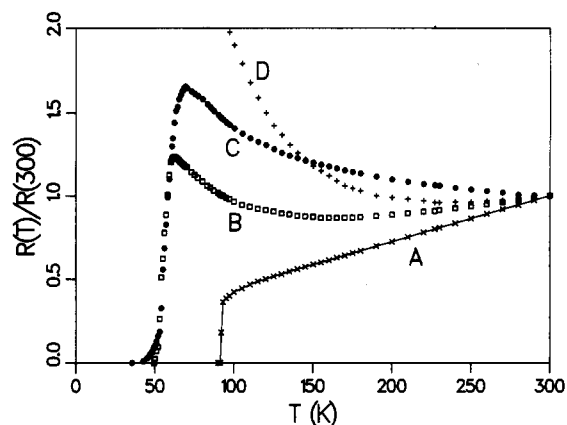


Figure 2. Normalized resistivity as a function of temperature for the orthorhombic phase (curve A) and three different samples of the tetragonal phase (curves B–D) of  $\text{YBa}_2\text{Cu}_3\text{O}_{7-x}$ .

tetragonal phase transition occurs in this material at ca  $750^\circ\text{C}$ .<sup>13</sup>

**X-ray Diffraction.**<sup>14</sup> Typical patterns of the tetragonal and orthorhombic phases (vide supra) are shown in Figure 1. The most notable differences are intensity redistributions around  $2\theta = 32.5, 47, 58$ , and  $68^\circ$  and peak splittings in the orthorhombic case, e.g., reflections (012) vs. (102). Lattice parameters were determined from the peak positions of 20–30 reflections. We find marked differences in the lattice constants depending on the annealing process. The tetragonal lattice constants (fast-cooled samples) are  $a = 3.8603(3)$  and  $c = 11.8255(3) \text{ \AA}$  (annealed in air) and  $a = 3.8648(5)$  and  $c = 11.7633(5) \text{ \AA}$  (annealed in  $\text{O}_2$ ). For the orthorhombic phase (slow-cooled samples) we find  $a = 3.826(2)$ ,  $b = 3.889(2)$ , and  $c = 11.673(4) \text{ \AA}$  when annealed in air, identical with those of the nonannealed material. Oxygen-annealed, slow-cooled orthorhombic phase material exhibits a qualitatively similar diffraction pattern but with broad, asymmetric peaks in which  $hkl$  and  $khl$  reflections coalesce. Lattice parameters of this material are  $a = 3.844(4)$ ,  $b = 3.889(4)$ , and  $c = 11.685(8) \text{ \AA}$ . The observed peak intensities for both orthorhombic and tetragonal phases are in good qualitative agreement with patterns simulated from the published structural data.<sup>7,8</sup>

**Electrical Properties.** The electrical resistances of small sections cut from pellets were measured by use of the four-lead technique with low-frequency ac currents and phase-sensitive detection. The temperature dependence of the resistances for one orthorhombic specimen (oxygen-annealed, slow-cooled material) and three different tetragonal phase specimens (all oxygen-annealed, fast-cooled material) is illustrated in Figure 2. Curve A in Figure 2 for the orthorhombic phase shows a linear decrease in resistance with decreasing temperatures from 300 K and then a sharp drop near 90 K to the superconducting state. The superconducting onset temperature (defined by the intersection of straight lines extrapolated from the normal-state resistance and from the sharp drop in resistance) occurred at 92.6 K. Zero resistance below instrument resolution occurred at 91.3 K, and the 10%–90% transition width was 1.0 K. The room-temperature resistivity,  $\rho$ , for this sample was estimated to be  $\rho(300 \text{ K}) \approx 1400 \mu\Omega \text{ cm}$ . These conductive properties compare favorably with those previously reported for the high- $T_c$  superconductor  $\text{YBa}_2\text{Cu}_3\text{O}_{7-x}$ .<sup>1-5</sup> We found very little variation in these properties from one orthorhombic sample to another (all oxygen-annealed, slow-cooled material).

The conductive properties of different tetragonal phase specimens (all oxygen-annealed fast-cooled material), however, exhibited considerable variation, although their X-ray powder

(13) Schuller, I. K.; Hinks, D. G.; Beno, M. A.; Capone, D. W., II; Soderholm, L.; Locquet, J.-P.; Bruynseraede, Y.; Segre, C. U.; Zhang, K. *Solid State Commun.*, in press.

(14) Norelco powder diffractometer,  $\text{Cu K}\alpha$  radiation ( $\lambda = 1.5418 \text{ \AA}$ ), monochromator on detector arm, calibrated with high purity Si. Typical scan parameters are  $1^\circ$  step width,  $0.025^\circ$  steps, and 5 s/step.

diffraction patterns were identical. Curves B-D in Figure 2 for three tetragonal samples show some partial metallic behavior over a limited range of temperature, along with semiconducting behavior at lower temperatures, and very broad superconducting transitions beginning below 70 K and finishing below 50 K. One sample (curve D), however, retained semiconductive behavior without a superconducting transition down to 15 K, which is the lowest temperature attained in these measurements. The room temperature resistivities of these three samples were estimated to be  $\sim 500$  (B), 13 000 (C), and 30 000  $\mu\Omega$  cm (D). While we cannot rule out the presence of a small amount of the orthorhombic phase (<5%) as being responsible for these anomalous conductive properties, we believe that these properties are due to different oxygen content in the tetragonal-phase samples. However, we do not find the tetragonal phase to be the 93 K superconductor.

In summary, we have demonstrated that, in the  $\text{YBa}_2\text{Cu}_3\text{O}_{7-x}$  superconductor sample, the cooling rate subsequent to oxygen annealing is a very critical factor in obtaining the high- $T_c$  superconducting orthorhombic phase.

**Acknowledgment.** Work at Argonne National Laboratory is sponsored by the Office of Basic Energy Sciences, Division of Materials Sciences, U.S. Department of Energy, under Contract W-31-109-Eng-38. We thank Ed Huff for the ICP/AES analysis and Dr. Mark Beno for helpful discussions. M.R.M. is a student research participant sponsored by the Argonne Division of Educational Programs from St. Michael's College, Winooski, VT.

Chemistry and Materials Science  
Divisions  
Argonne National Laboratory  
Argonne, Illinois 60439

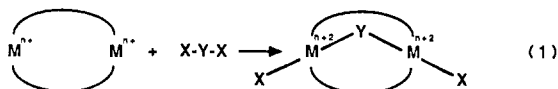
Aravinda M. Kini  
Urs Geiser  
Huey-Chuen I. Kao  
K. Douglas Carlson  
Hau H. Wang  
Marilyn R. Monaghan  
Jack M. Williams\*

Received April 23, 1987

### Three-Fragment, Two-Centered Oxidative Addition of $\text{AuCl}_4^-$ to $\text{Ir}_2(\text{CO})_2\text{Cl}_2[\mu-(\text{Ph}_2\text{PCH}_2)_2\text{AsPh}]_2$

Sir:

The two-center, three-fragment oxidative-addition reaction (eq 1) is relatively rare. The binuclear complex  $\text{Pd}_2(\text{dpm})_3$  (dpm is



bis(diphenylphosphino)methane) undergoes such reactions under both thermal<sup>1</sup> and photochemical<sup>2</sup> activation with a variety of organic dihalides including dihalomethanes, 1,2-diiodobenzene, dichlorophenyl isocyanide, and oxalyl chloride. Examples of the addition of dihalomethanes to a number of other metal complexes are also known.<sup>3</sup> Since the oxidative additions of metal-halogen bonds to a single metal center are known,<sup>4</sup> dihalometal complexes should also be able to participate (as  $\text{X}-\text{Y}-\text{X}$ ) in reaction 1. Here we report the first example of such a reaction, one in which  $\text{AuCl}_4^-$  acts as  $\text{X}-\text{Y}-\text{X}$  and two new metal-metal bonds are formed.

- (1) Balch, A. L.; Hunt, C. T.; Lee, C.-L.; Olmstead, M. M.; Farr, J. P. *J. Am. Chem. Soc.* **1981**, *103*, 3764.
- (2) Caspar, J. V. *J. Am. Chem. Soc.* **1985**, *107*, 6718.
- (3) Jandik, P.; Schubert, U.; Schmidbaur, H. *Angew. Chem.* **1982**, *94*, 74. Murray, H. H.; Fackler, J. P., Jr.; Mazany, A. M. *Organometallics* **1984**, *3*, 1310. El Amani, M.; Maisonnat, A.; Dahan, F.; Pince, R.; Poilblanc, R. *Organometallics* **1985**, *4*, 773. Werner, H.; Zolk, R. *Organometallics* **1985**, *4*, 601.
- (4) For examples see: Baker, R. W.; Braithwaite, M. J.; Nyholm, R. S. *J. Chem. Soc., Dalton Trans.* **1972**, 1924. Balch, A. L.; Olmstead, M. M. *J. Am. Chem. Soc.* **1976**, *98*, 2354. Olmstead, M. M.; Balch, A. L. *J. Organomet. Chem.* **1978**, *148*, C15. Farr, J. P.; Olmstead, M. M.; Balch, A. L. *J. Am. Chem. Soc.* **1986**, *108*, 6654.

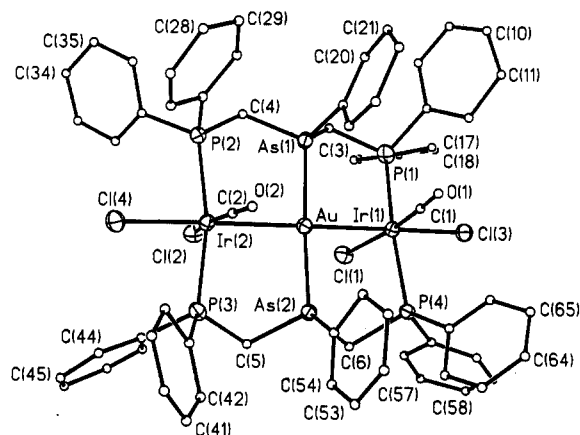
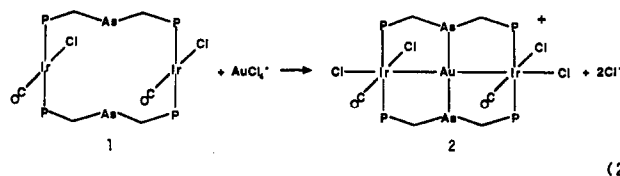


**Figure 1.** Perspective view of  $[\text{Ir}_2\text{Au}(\text{CO})_2\text{Cl}_4(\mu\text{-dpma})_2]^+$  showing 50% thermal ellipsoids for heavy atoms and arbitrarily sized, uniform circles for all carbon and oxygen atoms. Selected distances (Å) and angles (deg): Au-Ir(1), 2.812 (2); Au-Ir(2), 2.806 (2); Au-As(1), 2.379 (4); Au-As(2), 2.386 (4); Ir(1)-P(1), 2.390 (9); Ir(1)-P(4), 2.364 (9); Ir(1)-C(1), 1.88 (3); Ir(1)-Cl(1), 2.400 (7); Ir(1)-Cl(3), 2.455 (7); Ir(2)-P(2), 2.366 (10); Ir(2)-P(3), 2.366 (9); Ir(2)-C(2), 1.77 (3); Ir(2)-Cl(2), 2.395 (7); Ir(2)-Cl(4), 2.477 (8); Ir(1)-Au-Ir(2), 173.1 (1); As(1)-Au-As(2), 175.0 (1); As(1)-Au-Ir(1), 87.4 (1); As(1)-Au-Ir(2), 91.7 (1); As(2)-Au-Ir(1), 91.8 (1); As(2)-Au-Ir(2), 89.7 (1); P(1)-Ir(1)-P(4), 164.9 (3); Cl(1)-Ir(1)-C(1), 167 (1); Au-Ir(1)-Cl(3), 179.7 (2); P(2)-Ir(2)-P(3), 167.5 (3); Cl(2)-Ir(2)-C(2), 166.7 (9); Au-Ir(2)-Cl(4), 176.2 (2).

Addition of a yellow dichloromethane solution of  $[\text{Ph}_4\text{As}][\text{AuCl}_4]$  to a yellow solution of  $\text{Ir}_2(\text{CO})_2\text{Cl}_2(\mu\text{-dpma})_2$  (**1**) (dpma



is bis((diphenylphosphino)methyl)phenylarsine) produces a bright red solution from which red needles of  $[\text{Ir}_2\text{Au}(\text{CO})_2\text{Cl}_4(\mu\text{-dpma})_2]\text{Cl}$  (**2**) precipitate in 84% yield upon the addition of ethyl ether. The  $^{31}\text{P}$  NMR spectrum shows a singlet at  $\sim 8.4$  ppm (vs. 18.4 ppm for **1**). The infrared spectrum shows a terminal carbonyl absorption at  $2011\text{ cm}^{-1}$ . The increase in  $\nu(\text{CO})$  over that in **1** ( $1964\text{ cm}^{-1}$ ) is indicative of oxidation of iridium although the increase is rather small.<sup>6</sup>

The structure of **2** has been determined by an X-ray diffraction study.<sup>7</sup> A perspective view of the cation is shown in Figure 1. The chloride counterion, Cl(5), is not coordinated to the cation; the shortest Au...Cl(5) separation is  $6.41\text{ Å}$ . The cation has effective (noncrystallographic)  $C_{2v}$  symmetry with the 2-fold axis passing through the gold atom, perpendicular to the  $\text{Ir}_2\text{Au}(\text{C}-\text{O})_2\text{Cl}_4$  plane. The two iridium ions are six-coordinate while the gold ion is four-coordinate and planar. The positioning of Cl(3) and Cl(4) clearly shows that oxidative addition has occurred while the two arsenic atoms have replaced two of the chloride ions in the coordination of the gold ion. The Au-As distances (2.379 (4), 2.386 (4) Å) are similar to the Au-As distance in  $\text{Ph}_3\text{AsAuBr}$  (2.342 (5) Å).<sup>8</sup> The Au-Ir distances (2.812 (2), 2.806 (2) Å) are nearly equivalent and are just slightly longer than the range of other Au-Ir single bonds.<sup>9</sup> The coordination of the two iridium

- (5) Balch, A. L.; Fossett, L. A.; Olmstead, M. M.; Oram, D. E.; Reedy, P. E., Jr. *J. Am. Chem. Soc.* **1985**, *107*, 5272.
- (6) Vaska, L. *Acc. Chem. Res.* **1968**, *1*, 335.
- (7) Red crystals of  $[\text{Ir}_2\text{Au}(\text{CO})_2\text{Cl}_4(\mu\text{-dpma})_2]\text{Cl}$  were grown by diffusion of ethyl ether into a dichloromethane solution of **2**. They belong to the monoclinic space group  $P2_1/c$  (No. 14) with  $a = 13.346$  (2) Å,  $b = 12.794$  (5) Å,  $c = 44.82$  (3) Å,  $\beta = 98.29$  (4)° at 130 K with  $Z = 4$ . Refinement of 3106 reflections with  $I > 3\sigma(I)$  with 399 parameters yielded  $R = 0.0666$  and  $R_w = 0.0747$ .
- (8) Einstein, F. W. B.; Restivo, R. *Acta Crystallogr., Sect. B: Struct. Crystallogr. Cryst. Chem.* **1975**, *B31*, 624.